ORGANIC LETTERS

2012
Vol. 14, No. 4
960–963

(*S*)-ABOC: A Rigid Bicyclic β-Amino Acid as Turn Inducer

Christophe André,[⊥,†] Baptiste Legrand,[⊥,‡] Cheng Deng,[‡] Claude Didierjean,[§] Guillaume Pickaert,[‡] Jean Martinez,[†] Marie Christine Averlant-Petit,[‡] Muriel Amblard,[*,†] and Monique Calmes[†]

Institut des Biomolécules Max Mousseron (IBMM) UMR 5247 CNRS-UM1-UM2, Faculté de pharmacie, 15 Avenue Charles Flahault, 34093 Montpellier, France, Laboratoire de Chimie-Physique Macromoléculaire, UMR 7568 CNRS-Université de Lorraine, 1 rue Grandville, 54001 Nancy Cedex 1, France, and Laboratoire de Cristallographie, Résonance Magnétique et Modélisation, UMR 7036 CNRS-Université de Lorraine, Boulevard des Aiguillettes, 54506 Vandoeuvre-Lès-Nancy Cedex, France

muriel.amblard@univ-monpt1.fr

Received October 28, 2011

ABSTRACT

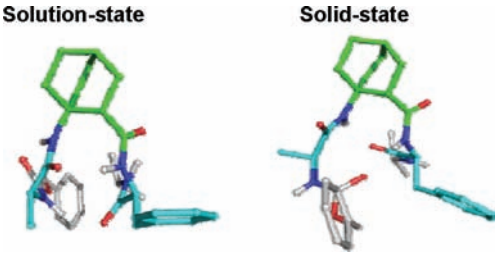

In order to investigate the ability of the (*S*)-aminobicyclo[2.2.2]octane-2-carboxylic acid 1 (H-(*S*)-ABOC-OH) to induce reverse turns into peptides, two model tripeptides, in which this bicyclic unit was incorporated into the second position, were synthesized and analyzed by FT-IR, CD, NMR, and X-ray studies.

The reverse-turn has long been recognized as a significant secondary structure element in globular protein architecture.[1] It is involved in protein folding[2] and constitutes an important site of molecular recognition in many biologically active peptides and proteins due to its frequent localization in the exposed surface.[3] Therefore, for more than 30 years, this small secondary structural element has been an attractive target to be mimicked by conformationally constrained motifs that are able to induce secondary structures found in peptides, proteins, or structural mimics thereof.[4] Most of these motifs are based on dipeptide mimetics.[4] However, β-amino acids that are mono- or di substituted on their 2- or 3-position have also been shown to induce turns in peptides. They were particularly applied to an important field of research that consists in the construction of small synthetic oligomers, called foldamers. Depending on the β-amino acid unit, various well-defined folding secondary structures, including a 14-, 12-, 10- and 8-helix, or even sheets were obtained.[5] With the

[⊥] The authors contributed equally to this work.

[†] Institut des Biomolécules Max Mousseron.
[‡] Laboratoire de Chimie-Physique Macromoléculaire, Nancy Université.
[§] Laboratoire de Cristallographie, Résonance Magnétique et Modélisation, Nancy Université.

(1) Richardson, J. S. *Adv. Protein Chem.* **1981**, *34*, 167.
(2) Marcelino, A. M.; Gierasch, L. M. *Biopolymers* **2008**, *89*, 380.
(3) (a) Kessler, H. *Angew. Chem., Int. Ed. Engl.* **1982**, *21*, 512. (b) Rose, G. D.; Gierasch, L. M.; Smith, J. A. *Adv. Protein Chem.* **1985**, *37*, 1. (c) Chou, K. C. *Anal. Biochem.* **2000**, *286*, 1. (d) Yin, H.; Hamilton, A. D. *Angew. Chem., Int. Ed.* **2005**, *44*, 4130.
(4) (a) Gillespie, P.; Cicariello, J.; Olson, G. L. *Biopolymers* **1997**, *43*, 191. (b) Hanessian, S.; McNaughton-Smith, G.; Lombart, H. G.; Lubell, W. D. *Tetrahedron* **1997**, *53*, 12789. (c) Amblard, M.; Daffix, I.; Bedos, P.; Berge, G.; Pruneau, D.; Paquet, J. L.; Luccarini, J. M.; Belichard, P.; Dodey, P.; Martinez, J. *J. Med. Chem.* **1999**, *42*, 4185. (d) North, M. *J. Pept. Sci.* **2000**, *6*, 301. (e) Cluzeau, J.; Lubell, W. D. *Biopolymers* **2005**, *80*, 98. (f) Robinson, J. A. *Acc. Chem. Res.* **2008**, *41*, 1278.
(5) (a) Gellman, S. H. *Acc. Chem. Res.* **1998**, *31*, 173. (b) Seebach, D.; Abele, S.; Sifferlen, T.; Hanggi, M.; Gruner, S.; Seiler, P. *Helv. Chim. Acta* **1998**, *81*, 2218. (c) Yang, D.; Qu, J.; Li, B.; Ng, F. F.; Wang, X. C.; Cheung, K. K.; Wang, D. P.; Wu, Y. D. *J. Am. Chem. Soc.* **1999**, *121*, 589. (d) Srinivas, D.; Gonnade, R.; Ravindranathan, S.; Sanjayan, G. J. *J. Org. Chem.* **2007**, *72*, 7022. (e) Wu, Y. D.; Han, W.; Wang, D. P.; Gao, Y.; Zhao, Y. L. *Acc. Chem. Res.* **2008**, *41*, 1418.

10.1021/ol203406v
Published on Web 01/31/2012

folding pattern being controlled by the monomeric motif forming the β-peptides, the search for new scaffolds able to modulate secondary structures appears to be of great potential use.[6] In this area, we have developed a research program for the selection of conformationally constrained motifs including β-turn mimics able to display well-defined secondary structures by oligomerization.[7] Among the different motifs that have been selected, we have focused on the (*S*)-aminobicyclo[2.2.2]octane-2-carboxylic acid **1** (H-(*S*)-ABOC-OH), a $\beta^{2,3,3}$-trisubstituted cyclic β-amino acid, as a potential turn inducer in peptides and a favorable scaffold to induce structured oligomers.

We have recently reported the asymmetric synthesis of this original rigid bicyclic β-amino acid **1** bearing an amino group at the bridgehead (Figure 1).[8] This compound is particularly attractive because it combines both the structural properties of constrained cyclic compounds and those of β-amino acids, which have been intensively used as foldamer precursors.[5a]

The high level of constraint of the (*S*)-ABOC motif, with all adjacent methylene protons eclipsed and its carboxylic acid and amino groups in a synclinal conformation, provides a template with drastically reduced conformational freedom. This feature should allow a high degree of conservation of ABOC angles when incorporated into peptide/protein sequences or foldamer compounds. The crystal structure of Boc derivative **2** is represented in Figure 1.

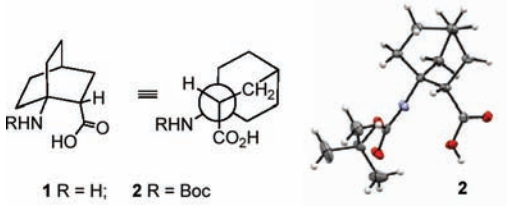

Figure 1. Crystal structure of the Boc-(*S*)-ABOC-OH **2**.

To further explore its properties, we decided to synthesize and study the conformational behavior of two model tripeptides **3** and **4** incorporating the constrained ABOC in the central position, by means of CD, FT-IR, NMR spectroscopies and XR diffraction. Their syntheses were performed following the standard Boc protecting group synthesis of peptides strategy in solution (Scheme 1).

We then investigated the structural features of **3** and **4** in solution using several spectral analyses. Experiments were carried out in $CDCl_3$ or in CD_3CN in accordance with the peptide solubility and solvent transparency, i.e. $CDCl_3$ for infrared spectroscopy, CD_3CN to record circular dichroism spectra, and both solvents for NMR studies. No significant differences were observed in NMR spectra in $CDCl_3$ or in CD_3CN (Figure S3A−L and Tables S4 and S5). In addition, FT-IR and NMR data of **3** and **4** were compared to those obtained for a control tripeptide Z-Ala-β-Ala-Phe-NHiPr **10** containing an unconstrained β-amino acid replacing the rigid ABOC residue.

Scheme 1. Synthesis of Tripeptides **3** and **4**

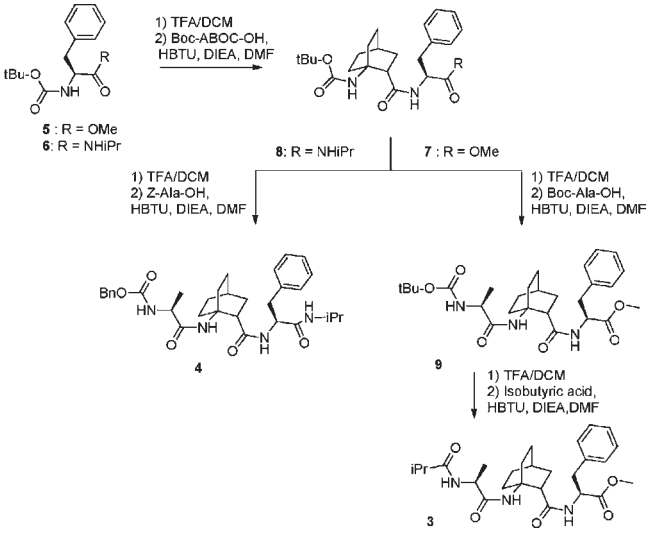

The extent of hydrogen bonding in **3** and **4** in $CDCl_3$ was evaluated through FT-IR spectroscopy experiments (Figure S1 A−H), DMSO-titration NMR experiments, and temperature coefficients of amide protons in the 283 to 313 K range (Figure S5).

First, the solvent accessibility of the NH proton resonances was measured by a DMSO-titration experiment with gradual addition of DMSO-d_6 to the $CDCl_3$ solution (Figure S4). It can be assumed that low temperature coefficients in DMSO-d_6 (< 5 ppb/K) are related to inaccessible protons to the solvent and lower values in $CDCl_3 \leq 2.4$ ppb/K are related not only to shielded protons (which remained shielded over the temperature range) but also to accessible ones. Accordingly only temperature coefficients significantly larger than 2.4 ppb/K in $CDCl_3$ can be unambiguously assigned to NH protons initially shielded, which become exposed to the solvent in the course of the temperature range.[9]

A similar behavior was observed for the tripeptides **3** and **4**. First, the large NH(Ala) temperature coefficient values for **3** and **4** (4.4 and 5.2 ppb/K) in $CDCl_3$ associated to weak chemical shift variations with the addition of DMSO-d_6 (0.87 and 0.45 ppm) suggested solvent accessibility. In contrast, the NH(ABOC) and NH(Phe) exhibited low temperature coefficients in $CDCl_3$ (1.4 and 3.0 ppb/K for **3** and 0.9 and 1.0 ppb/K for **4**). The conformational stability imposed by the ABOC motif should influence these temperature coefficients.

(6) Rathore, N.; Gellman, S. H.; de Pablo, J. J. *Biophys. J.* **2006**, *91*, 3425.

(7) Raynal, N.; Averlant-Petit, M. C.; Berge, G.; Didierjean, C.; Marraud, M.; Duru, C.; Martinez, J.; Amblard, M. *Tetrahedron Lett.* **2007**, *48*, 1787.

(8) Songis, O.; Didierjean, C.; Laurent, C.; Martinez, J.; Calmes, M. *Eur. J. Org. Chem.* **2007**, 3166.

(9) (a) Llinas, M.; Klein, M. P. *J. Am. Chem. Soc.* **1975**, *97*, 4731. (b) Stevens, E. S.; Sugawara, N.; Bonora, G. M.; Toniolo, C. *J. Am. Chem. Soc.* **1980**, *102*, 7048. (c) Medda, A. K.; Park, C. M.; Jeon, A.; Kim, H.; Sohn, J. H.; Lee, H. S. *Org. Lett.* **2011**, *13*, 3486.

Despite border temperature coefficients in DMSO-d_6, small chemical shift variations (around 1 ppm) along the DMSO-titration experiments indicated the participation of these amide protons in an intramolecular hydrogen bond. Finally, all measured parameters for the additional NH(iPr) in **4**, i.e. small temperature coefficient in $CDCl_3$, large value in DMSO-d_6, and large chemical shift difference between $CDCl_3$ and DMSO-d_6 (ΔNH = 2.16 ppm), indicated a solvent-accessible NH proton.

To gain further information on the hydrogen bond network, FT-IR spectroscopy studies were undertaken. As previously mentioned, frequencies of amide A and amide I bands corresponding to NH and CO stretching vibrations, respectively, depend on the involvement of vibrators in hydrogen bonds.[10] Typically, the frequencies of stretching vibrations decrease with hydrogen bonding formation. Those of the hydrogen bonded NH and CO amide rise below 3400 and 1680 cm,$^{-1}$ respectively, and overlaps between "bound" and "free" bands are common in the latter case. Moreover, with the time scale of infrared spectroscopy being faster than that of NMR, an infrared spectrum can contain the spectral contributions of all components of a pool of conformers.[11] Thus, for the same CO or NH function, it should be possible to see both the bonded and nonbonded forms.

In order to assign the positions of free NH and CO vibrators of tripeptides **3** and **4**, we first studied precursors **6**, **7**, **8**, and **9** (Tables S1 and S2 and Figure S1A–D). For these precursors, we found no evidence of strong bonded NH absorption bands as could be observed in the intramolecular reverse turn or in intermolecular interactions.[12] However, the (*S*)-ABOC motif led to a new band at 3398 cm^{-1} in precursor **8**, suggesting a certain contribution of H-bonded species (Figure S1A). In the case of **4** a broad band at 3295 cm^{-1} suggested the existence of a stronger hydrogen-bonding interaction and therefore a higher level of structuration (Figure S1A). No distinguishable band around 3300 cm^{-1} was observed for **3**, but an enlargement of the signal suggested an emergent hydrogen bond (Figure S1B). Nevertheless for this tripeptide, a shoulder around 1655 cm^{-1} corresponding to a hydrogen bonded CO stretch was present (Figure S1D). The study of CO stretching vibrations of all compounds showed either a global shift of vibrators to lower frequencies or shoulders, both related to bonded carbonyls. Both FT-IR amide A and amide I band analyses of **3** and **4** confirmed the involvement of NH and CO groups in hydrogen-bonding interactions. In addition, comparison of **10** with **4** showed a higher level of structuration for the latter. Indeed, in the amide A region (Figure S1G), **4** revealed a NH bonded band at a lower frequency (3295 cm^{-1}) than **10**, which showed a major band at 3343 cm^{-1} and a shoulder at 3300 cm^{-1}. Moreover, the ratio of the integrated intensity of the hydrogen-bonded NH bands to free NH bands (A_H/A_F)[13] was much higher in the case of the ABOC containing tripeptide (A_H/A_F = 1.94) than in the case of the β-Ala analog (A_H/A_F = 0.89). This suggested a higher involvement of NH groups in intramolecular interactions in **4** compared to **10**. Finally, in the amide I region (Figure S1H), a free CO band at 1675 cm^{-1} was only observed for **10**, which confirmed the previous observations of a higher structuration level for **4**.

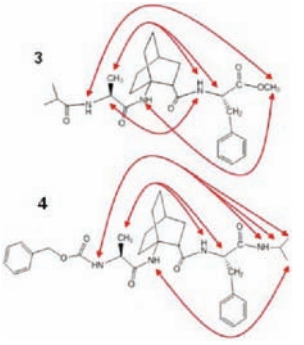

Figure 2. ROE long-range distances (red arrows) in $CDCl_3$ at 298 K for **3** and **4**.

To gain more insight into the conformation of compounds **3** and **4** in solution, we recorded CD spectra in CD_3CN and performed NMR studies based on ROESY spectra (10 mM, 298 K) in $CDCl_3$ and CD_3CN. As no signal could be detected for **2**, the similar CD spectra of **3** and **4** with a maximum around 220 nm could indicate the presence of comparable structuration (Figure S2). For both compounds, ROE derived distances as upper bound distances were used for structural calculations (Table S7). The ROE long-range distances in $CDCl_3$ are reported in Figure 2. For the structure calculations using AMBER10, 21 and 19 distance restraints for **3** and 22 and 20 distance restraints for **4** in $CDCl_3$ and CD_3CN respectively were introduced. As expected, the set of ROEs observed on the ROESY spectra were very close for **3** and **4** in both solvents. The characteristic ROE long-range distances between protons on each side of the ABOC residue suggested a reverse turn scaffold for both compounds. The 15 lowest energy structures of **3** and **4** in $CDCl_3$ and CD_3CN are reported in Figure S6. As indicated, the root-mean-square deviations (rmsd) fit on backbone heavy atoms were very low in the four calculated sets of structures and decreased significantly when the terminal flexible moieties were omitted (rmsd around 0.2). Indeed, we noticed that the backbone trace of Ala-(*S*)-ABOC-Phe was particularly

(10) (a) Byler, D. M.; Susi, H. *Biopolymers* **1986**, *25*, 469. (b) Arrondo, J. L. R.; Muga, A.; Castresana, J.; Goni, F. M. *Prog. Biophys. Mol. Biol.* **1993**, *59*, 23. (c) Vass, E.; Hollosi, M.; Besson, F.; Buchet, R. *Chem. Rev.* **2003**, *103*, 1917.

(11) Vass, E.; Kurz, M.; Konat, R. K.; Hollosi, M. *Spectrochim. Acta, Part A* **1998**, *54*, 773.

(12) (a) Chung, Y. J.; Huck, B. R.; Christianson, L. A.; Stanger, H. E.; Krauthauser, S.; Powell, D. R.; Gellman, S. H. *J. Am. Chem. Soc.* **2000**, *122*, 3995. (b) Allix, F.; Curcio, P.; Quoc, N. P.; Pickaert, G.; Jamart-Gregoire, B. *Langmuir* **2010**, *26*, 16818.

(13) (a) Benedetti, E.; Bavoso, A.; Di Baso, B.; Pavone, V.; Pedone, C.; Crisma, M.; Bonora, G. M.; Toniolo, C. *J. Am. Chem. Soc.* **1982**, *104*, 2437. (b) Bonora, G. M.; Mapelli, C.; Toniolo, C.; Wilkening, R. R.; Stevens, E. S. *Int. J. Biol. Macromol.* **1984**, *6*, 179.

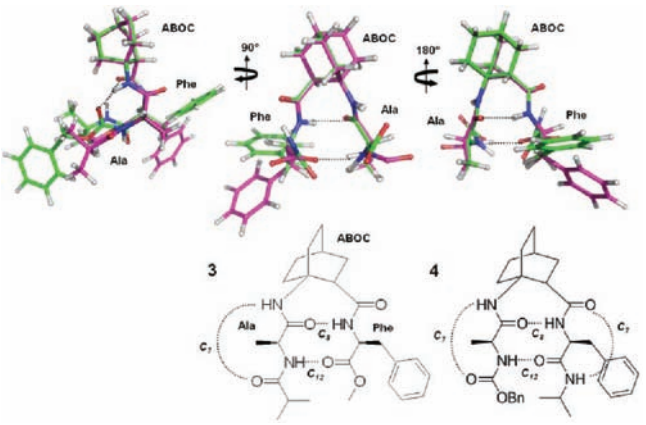

Figure 3. Overlay of **3** (magenta) and **4** (green) average NMR solution structures in $CDCl_3$ and representation of the (*S*)-ABOC-driven reverse turn. H-bonds are shown as dashed lines.

well-defined in a reverse turn conformation in $CDCl_3$ and CD_3CN. Figure 3 showed that **3** and **4** share similar conformations retained in both solvents. For compound **10**, 21 distance restraints were used for structure calculation but only two long-range NOEs could be detected in the ROESY spectrum in $CDCl_3$. Indeed while, for **4**, typical NOEs involved the NH(Ala) and the NH, CH, or CH_3 of the C-terminal NHiPr group, none of them could be detected for **10**. As a result, the rmsd fit on backbone heavy atoms for this compound was higher than that of **3** and **4** (0.429 for **10** vs 0.160 and 0.131 for **3** and **4** respectively) indicating significant structural discrepancies among the NMR lowest energy structures despite a global turn shape (Figure S6E). The significant standard deviation on the dihedral angle values also underlined the higher conformational freedom of the tripeptide **10** in comparison to **3** and **4** (Table S8).

For compounds **3** and **4** the turn was stabilized by two hydrogen bonds, between the NH(Phe) and CO(Ala) and the NH(Ala) and CO(Phe), which formed a "C_8" and a "C_{12}" pseudocycle respectively. In addition, "C_7 lateral pseudocycles" were stabilized by hydrogen bonds between the NH(ABOC) and CO(N-ter) for **3** and **4** and the NH-(iPr) and CO(ABOC) for **4**.

The crystals obtained in CH_2Cl_2 by slow evaporation allowed us to obtain the solid state structure of the tripeptide **4** (Figure 4). We noticed that this peptide also adopted a turn in the crystal but with a different hydrogen bond network. In the crystal, two hydrogen bonds were present between the NH(ABOC) and the CO(Phe), and the NH(Phe) and CO(Z) forming a "C_9" and a "C_{11}" pseudocycle. However, as observed in Figure 4, the reverse turn global conformation in the solid state and solution were almost superimposed. The main difference was the position of the benzyl moiety rotated toward the phenylalanine side chain in the solid state (Figure S7), which was, however, incompatible

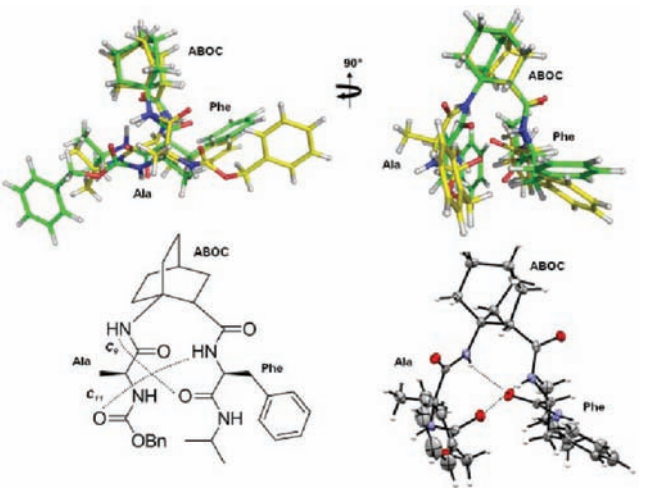

Figure 4. Overlay of crystal structure (yellow) and average NMR solution structure (green) in $CDCl_3$ of **4**. H-bonds are shown as dashed lines.

with the long-range ROEs previously described in solution (especially between the NH(Ala) and the isopropyl group).

To further compare the (*S*)-ABOC turn in solution and in the solid state, the backbone torsion angles ϕ, ψ, and θ were determined (Table S8). As expected, backbone torsion angles of compounds **3** and **4** were similar. The characteristic θ angle value of the (*S*)-ABOC β-residue was $\sim 50°-60°$. The variation of the benzyl urethane group position in solution and in the solid state was associated to rotations of the alanine ϕ and ψ dihedral angles (i.e., $-88.7°$ vs $-48.9°$ and $31.1°$ vs $142.2°$ in solution and in the crystal, respectively). The preferred conformation in the crystal was stabilized by the CO(Z)-NH(Phe) hydrogen bond. Nevertheless, in tripeptide **4**, despite discrepancies in the hydrogen bond network, other angles exhibited relatively close values in solution and in the crystal.

In this paper, we developed a novel reverse turn scaffold based on the β-residue (*S*)-ABOC conformationally restrained motif. We described its ability to induce a highly stable turn in solution. Thus, it constitutes a new building block to design original larger ABOC-based oligomers providing original secondary structures (e.g., helices).

Acknowledgment. The authors thank the CNRS, MESR, and ANR (ANR-08-BLAN-0066-01) for financial support, the SCBIM and service commun de cristallographie of Université de Lorraine for NMR and XRD facilities, and Mr E. Wenger for RX experiments.

Supporting Information Available. Experimental procedure, FT-IR, CD spectra, NMR structural calculations and crystal data. This material is available free of charge via the Internet at http://pubs.acs.org.

The authors declare no competing financial interest.